

# Unprecedented $\eta^1$ - $P_{basal}$ Coordination of $P_4X_3$ Molecules ( $X = S, Se$ ). An Experimental and Theoretical Study of the Apical vs Basal Complexation Dichotomy

Elisabetta Guidoboni,<sup>†</sup> Isaac de los Rios,<sup>‡</sup> Andrea Ienco,<sup>‡</sup> Lorenza Marvelli,<sup>†</sup> Carlo Mealli,<sup>\*†</sup> Antonio Romerosa,<sup>§</sup> Roberto Rossi,<sup>\*†</sup> and Maurizio Peruzzini<sup>\*†</sup>

Laboratorio di Chimica Nucleare ed Inorganica, Dipartimento di Chimica, Università di Ferrara, Via L. Borsari 46, 44100 Ferrara, Italy, ISSECC-CNR, V. Jacopo Nardi 39, 50132, Florence, Italy, and Área de Química Inorgánica, Facultad de Ciencias, Universidad de Almería, Almería, Spain

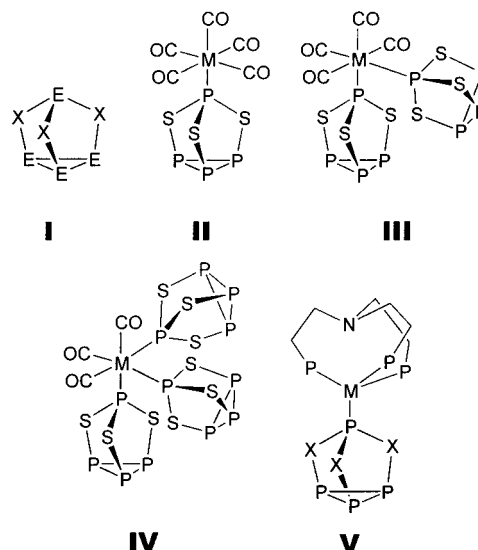
Received May 25, 2001

Reaction of [(triphos)Re(CO)<sub>2</sub>(OTf)] (**1**) [triphos = MeC(CH<sub>2</sub>PPh<sub>2</sub>)<sub>3</sub>; OTf = OSO<sub>2</sub>CF<sub>3</sub>] with P<sub>4</sub>S<sub>3</sub> and P<sub>4</sub>Se<sub>3</sub> yields pairs of coordination isomers, namely, [(triphos)Re(CO)<sub>2</sub>{ $\eta^1$ - $P_{apical}$ -P<sub>4</sub>X<sub>3</sub>}]<sup>+</sup> ( $X = S, 2$ ; Se, **5**) and [(triphos)Re(CO)<sub>2</sub>{ $\eta^1$ - $P_{basal}$ -P<sub>4</sub>X<sub>3</sub>}]<sup>+</sup> ( $X = S, 3$ ; Se, **6**). The latter represent the first examples of the  $\eta^1$ - $P_{basal}$  coordination achieved by the P<sub>4</sub>X<sub>3</sub> molecular cage. Further reaction of **2/3** and **5/6** mixtures with **1** affords the dinuclear species [(triphos)Re(CO)<sub>2</sub>]<sub>2</sub>{ $\mu, \eta^{1:1}$ - $P_{apical}, P_{basal}$ -P<sub>4</sub>X<sub>3</sub>}]<sup>2+</sup> ( $X = S, 4$ ; Se, **7**) in which the unprecedented M- $\eta^1$ - $P_{basal}/\eta^1$ - $P_{apical}$ -M' bridging coordination of the P<sub>4</sub>X<sub>3</sub> molecule is accomplished. A theoretical analysis of the bonding properties of the two coordination isomers is also presented. The directionality of apical vs basal phosphorus lone pairs is also discussed in terms of MO arguments.

## Introduction

The neutral mixed-cage molecules E<sub>4</sub>X<sub>3</sub> (E = P, As; X = S, Se) exhibit a unique and fascinating structure formed by a tetrahedral array of pnictogen atoms with a homocyclic-E<sub>3</sub> unit connected via three bridging chalcogen atoms to a single pnictogen atom in apical position (**I**).<sup>1</sup> The behavior of these molecules as ligands toward transition metal species has been widely studied, and a variety of modular pathways approaching the disruptive fragmentation of the heptatomic cages, particularly P<sub>4</sub>S<sub>3</sub> and As<sub>4</sub>S<sub>3</sub>, have been documented.<sup>2–5</sup>

The primary complexation of these molecules has also been accomplished, but the known compounds in which an intact, not activated, E<sub>4</sub>X<sub>3</sub> molecule behaves as a two-electron



ligand toward a transition metal fragment are still scarce. Such a topology, which requires a Lewis acid metal center, has been accomplished in octahedral complexes, e.g., [M(CO)<sub>5-x</sub>( $\eta^1$ -P<sub>4</sub>S<sub>3</sub>)<sub>1+x</sub>] [M = Mo, W, x = 0 (**II**);<sup>6</sup> M = Cr, Mo, W, x = 1 (**III**);<sup>7</sup> M = Cr, Mo, x = 2 (**IV**)<sup>7</sup>] as well as in tetrahedral ones, e.g., [(NP<sub>3</sub>)M( $\eta^1$ -P<sub>4</sub>X<sub>3</sub>)] (**V**) [NP<sub>3</sub> =

\* Authors to whom correspondence should be addressed. E-mail: peruz@fi.cnr.it (M.P.).

<sup>†</sup> Università di Ferrara.

<sup>‡</sup> ISSECC-CNR.

<sup>§</sup> Universidad de Almería.

(1) Riess, J. G. In *Rings, Cluster, and Polymers*; Cowley, A. H., Ed.; ACS Symposium Series 232; American Chemical Society: Washington, DC, 1983; p 17.

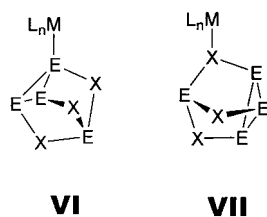
(2) Di Vaira M.; Stoppioni P.; Peruzzini M. *Comments Inorg. Chem.* **1990**, *11*, 1.

(3) Di Vaira M.; Stoppioni P. *Coord. Chem. Rev.* **1992**, *120*, 259.

(4) Wachter, J. *Angew. Chem., Int. Ed.* **1998**, *37*, 751.

(5) Goh, L. Y. *Coord. Chem. Rev.* **1999**, *185/186*, 257.

$N(\text{CH}_2\text{CH}_2\text{PPh}_2)_3$ ;  $M = \text{Ni}, \text{Pd}$ ;  $X = \text{S}, \text{Se}$ ).<sup>8,9</sup> In all of the latter compounds, characterized by either X-ray diffraction analysis<sup>6,8–10</sup> or <sup>31</sup>P NMR spectroscopy,<sup>7</sup> the cage molecule is bonded to the organometallic fragment through the lone pair of the apical phosphorus atom (**VI–V**). Also, 1:2 inclusion complexes  $[\{\text{P}_4\text{X}_3\}\{\text{Ni}(\text{TMTAA})\}_2]$  [ $\text{TMTAA} = 5,7,12,14$ -tetramethyldibenzo[*b,i*]-[1,4,8,11]tetrazacyclotetradecinenickel(II)] have been recently characterized by crystallographic methods.<sup>11,12</sup> In keeping with the observed reactivity, the apical P-donor of the  $\text{P}_4\text{S}_3$  molecule assimilates to a tertiary phosphine whereas the basal P atoms behave like the triangular *cyclo*- $\text{P}_3$  unit of one  $\text{P}_4$  molecule.<sup>13</sup> Also, the chalcogen atoms could have coordination capabilities toward thiophilic and selenophilic organometallic fragments.<sup>14</sup> Therefore, it is surprising that  $\text{P}_4\text{X}_3$ -transition metal complexes featuring either metal-to- $\text{P}_{\text{basal}}$  (**VI**) or metal-to-chalcogen coordination modes (**VII**) have not yet been described.



In this paper we report on the synthesis and characterization of some rhenium(I) derivatives of  $\text{P}_4\text{S}_3$  and  $\text{P}_4\text{Se}_3$  which in solution exist as a mixture of  $\text{Re}-\eta^1\text{-P}_{\text{apical}}$  and  $\text{Re}-\eta^1\text{-P}_{\text{basal}}$  coordination isomers. Remarkably, the latter coordination mode is unprecedented. Moreover, we provide the first and clear-cut evidence of dinuclear compounds which combine the  $M-\eta^1\text{-P}_{\text{basal}}$  and  $M'-\eta^1\text{-P}_{\text{apical}}$  coordination modes. In the latter compounds, an intact  $\text{P}_4\text{X}_3$  molecule is sandwiched between two organometallic fragments.

The electronic nature of the two possible monometallic isomers has been analyzed, and the most significant results have been discussed.

## Results and Discussion

The octahedral complex  $[(\text{triphos})\text{Re}(\text{CO})_2(\text{OTf})]$  (**1**)<sup>15</sup> [ $\text{triphos} = \text{MeC}(\text{CH}_2\text{PPh}_2)_3$ ;  $\text{OTf} = \text{OSO}_2\text{CF}_3$ ] readily

dissociates triflate in the presence of a variety of two-electron-donor ligands to yield the adducts  $[(\text{triphos})\text{Re}(\text{CO})_2(\text{L})]^n+$  [ $n = 1, \text{L} = \text{H}_2$ ,<sup>16</sup>  $\text{CO}$ ,<sup>16</sup>  $\text{CNR}$ ,<sup>15</sup>  $\text{HCCR}$ ,<sup>17</sup> carbene,<sup>17,18</sup> vinylidene,<sup>17,18</sup> allenylidene,<sup>17,18</sup>  $\text{THF}$ ,<sup>20</sup>  $\text{CH}_3\text{CHO}$ ,<sup>20</sup>  $\text{RSH}$ ,<sup>20</sup>  $\text{H}_2\text{S}$ ,<sup>21</sup>  $\text{P}_4$ ,<sup>22</sup>  $n = 0, \text{L} = \text{H}$ ,<sup>16</sup> halide,<sup>15,16</sup> pseudohalide,<sup>15</sup>  $\sigma$ -organyl<sup>17–19</sup>]. Particularly interesting for the present study is the reaction of **1** with white phosphorus, which yields the stable  $\eta^1\text{-P}_4$  complex  $[(\text{triphos})\text{Re}(\text{CO})_2(\eta^1\text{-P}_4)](\text{OTf})$  in excellent yield.<sup>22</sup> In view of the latter result, the reactivity of **1** has been tested also toward the  $\text{P}_4\text{X}_3$  cages ( $X = \text{S}, \text{Se}$ ).

**Synthesis and Characterization of the Coordination Isomers of  $\text{P}_4\text{S}_3$ .** At room temperature, **1** readily reacts in  $\text{CH}_2\text{Cl}_2$  with 1 molar equiv of  $\text{P}_4\text{S}_3$ , producing a pale yellow solution. Upon concentration of the solution under vacuum, a microcrystalline solid may be isolated in fairly good yield. The elemental analysis of the reaction crude confirms the formation of the expected 1:1 adduct between the  $[(\text{triphos})\text{Re}(\text{CO})_2]^+$  synthon and the  $\text{P}_4\text{S}_3$  molecule (Scheme 1).

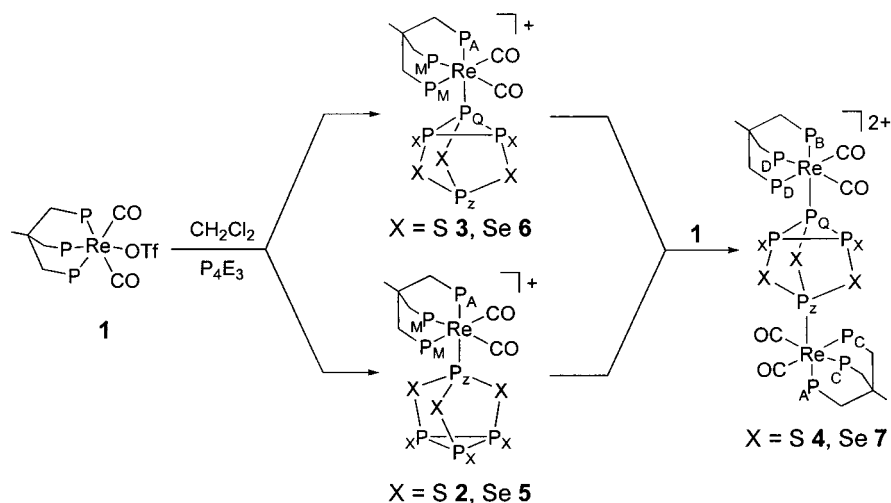
<sup>31</sup>P{<sup>1</sup>H} NMR spectroscopy of the reaction product in  $\text{CD}_2\text{-Cl}_2$  indicates the presence of two species in the approximate ratio 1:7. The latter are interpreted as a pair of coordination isomers differing for the bonding mode of the  $\text{P}_4\text{S}_3$  ligand, namely,  $[(\text{triphos})\text{Re}(\text{CO})_2\{\eta^1\text{-P}_{\text{apical}}\text{-P}_4\text{S}_3\}]^+$  (**2**) and  $[(\text{triphos})\text{Re}(\text{CO})_2\{\eta^1\text{-P}_{\text{basal}}\text{-P}_4\text{S}_3\}]^+$  (**3**) (Scheme 1). The relevant NMR parameters are listed in Table 1 together with the labeling scheme adopted to identify the different phosphorus nuclei. A comparison of the NMR properties of the coordinated and uncoordinated  $\text{P}_4\text{X}_3$  cage molecules is provided in Table 2 and highlights the similarities and the differences in the two series of complexes.

The less abundant isomer displays an  $\text{AM}_2\text{X}_3\text{Z}$  splitting pattern consistent with the formulation  $[(\text{triphos})\text{Re}(\text{CO})_2\{\eta^1\text{-P}_{\text{apical}}\text{-P}_4\text{S}_3\}]^+$  (**2**) in which the cage, responsible for the  $\text{X}_3\text{Z}$  part of the spin system, is coordinated to the metal via the apical phosphorus atom. This has usually been found for the few known coordination compounds containing an intact molecule of tetraphosphorus trisulfide as a ligand.<sup>6–9</sup> Noticeably, the rhenium-bonded  $\text{P}_Z$  atom falls at  $\delta$  91.52 as a slightly broadened doublet of pseudosextuplets. The large separation between the two components of the multiplet is due to the strong coupling of  $\text{P}_Z$  with the trans-disposed triphos phosphorus atom,  $\text{P}_A$  ( $^2J_{AZ}$  147.5 Hz), while the observed pseudosextuplet multiplicity arises from similar values of the geminal couplings involving the cis-disposed triphos  $\text{P}_M$  atoms ( $^2J_{MZ}$  25.5 Hz) and the three equivalent  $\text{P}_X$

- (6) Cordes, A. W.; Joyner, R. D.; Shores, R. D.; Dill, E. D. *Inorg. Chem.* **1974**, *13*, 132.
- (7) Jefferson, R.; Klein, H. F.; Nixon, J. F. *J. Chem. Soc., Chem. Commun.* **1969**, 536.
- (8) Di Vaira, M.; Peruzzini, M.; Stoppioni, P. *Inorg. Chem.* **1983**, *22*, 2196.
- (9) Di Vaira, M.; Peruzzini, M.; Stoppioni, P. *J. Organomet. Chem.* **1983**, *258*, 373.
- (10) The existence of  $[\text{Cr}(\text{CO})_5(\eta^1\text{-As}_4\text{S}_3)]$  has also been briefly mentioned. See footnote 92 in ref 4.
- (11) Andrews, P. C.; Atwood, J. L.; Barbour, L. J.; Nichols, P. J.; Raston, C. L. *Chem. Eur. J.* **1998**, *4*, 1384.
- (12) Andrews, P. C.; Atwood, J. L.; Barbour, L. J.; Croucher, P. D.; Nichols, P. J.; Smith, N. O.; Skelton, B. W.; White, A. H.; Raston, C. L. *J. Chem. Soc., Dalton Trans.* **1999**, 2927.
- (13) Head, J. D.; Mitchell, K. A. R.; Noodleman, L.; Paddock, N. L. *Can. J. Chem.* **1977**, *55*, 669.
- (14) Sulfur coordination of  $\text{P}_4\text{S}_3$  has been postulated by Riess in the reaction of the cage molecule with  $[\text{M}(\text{CO})_5(\text{thf})]$  in THF on the basis of in situ NMR analysis (see ref 1). However, in our hands, this result could not be confirmed at least in the case of  $[\text{Mo}(\text{CO})_5(\text{thf})]$ .
- (15) Bergamini, P.; Fabrizi De Biani, F.; Marvelli, L.; Mascellani, N.; Peruzzini, M.; Rossi, R.; Zanello, P. *New J. Chem.* **1999**, 207.

- (16) Bianchini, C.; Marchi, A.; Marvelli, L.; Peruzzini, M.; Romerosa, A.; Rossi, R.; Vacca, A. *Organometallics* **1995**, *14*, 3203.
- (17) Bianchini, C.; Marchi, A.; Marvelli, L.; Peruzzini, M.; Romerosa, A.; Rossi, R. *Organometallics* **1996**, *15*, 3804.
- (18) Bianchini, C.; Mantovani, N.; Marchi, A.; Marvelli, L.; Masi, D.; Peruzzini, M.; Rossi, R.; Romerosa, A. *Organometallics* **1999**, *18*, 4501.
- (19) Bianchini, C.; Mantovani, N.; Marvelli, L.; Peruzzini, M.; Rossi, R.; Romerosa, A. *J. Organomet. Chem.* **2001**, *617/618*, 233.
- (20) Peruzzini, M.; Rossi, R. Unpublished results.
- (21) Peruzzini, M.; de los Rios, I.; Romerosa, A. *Prog. Inorg. Chem.* **2001**, *49*, 169.
- (22) Peruzzini, M.; Marvelli, L.; Romerosa, A.; Rossi, R.; Vizza, F.; Zanobini, F. *Eur. J. Inorg. Chem.* **1999**, 931.

## Scheme 1



atoms of the P<sub>4</sub>S<sub>3</sub> basal unit (<sup>2</sup>*J*<sub>XZ</sub> 23.4 Hz). An inset expanding this multiplet is provided as trace a in Figure 1.

In keeping with the proposed structure, the three basal P<sub>X</sub> atoms give a broad doublet with only a discernible coupling to the apical P<sub>Z</sub> phosphorus atom (trace d in Figure 1). The triphos resonances, which for third-row transition metal complexes<sup>15–19,22</sup> fall slightly upfield with respect to the H<sub>3</sub>-PO<sub>4</sub> reference, exhibit multiplicities and coupling constants consistent with the presence of the  $\eta^1$ -*P*<sub>apical</sub>-P<sub>4</sub>S<sub>3</sub> ligand. The broadness of the resonances due to the phosphorus atoms of the  $\eta^1$ -*P*<sub>apical</sub>-P<sub>4</sub>S<sub>3</sub> ligand is not easily explained. Remarkably, the line widths of these signals do not change appreciably on lowering the temperature of the CD<sub>2</sub>Cl<sub>2</sub> solution down to –60 °C.<sup>23</sup> Accordingly, the only dynamic process must be a fast rotation of the cage about its symmetry axis which cannot be blocked even at the lowest accessible temperature.

The major component of the reaction mixture exhibits an AM<sub>2</sub>QX<sub>2</sub>Z spin system which agrees with the formation of the coordination isomer [(triphos)Re(CO)<sub>2</sub>{ $\eta^1$ -*P*<sub>basal</sub>-P<sub>4</sub>S<sub>3</sub>}]<sup>+</sup> (**3**). Namely, the heptatomic cage is coordinated to rhenium atom through one basal phosphorus atom. The breaking of the 3-fold symmetry in the P<sub>4</sub>S<sub>3</sub> molecule determines the most intriguing feature in the NMR spectrum of **3**, i.e., the appearance in the high-field part of the spectrum of two well-separated resonances with an intensity ratio of 1:2. The less intense signal, trace c in Figure 1, at  $\delta$  –44.16, is assigned to the unique phosphorus atom bonded to the metal (P<sub>O</sub>) while the other resonance at  $\delta$  –134.17, trace e in Figure 1, corresponds to the two nonmetalated basal phosphorus atoms P<sub>X</sub>. The latter signal is moderately shielded with respect to the three equivalent basal P atoms in **2** [ $\Delta = \delta(\text{P}_X)_3 - \delta(\text{P}_X)_2 = 15.6$  ppm] as well as to free P<sub>4</sub>S<sub>3</sub><sup>24</sup> [ $\Delta = \delta(\text{P}_X)_3 - \delta(\text{P}_X)_{\text{P}_4\text{S}_3} = 6.8$  ppm] and is characterized by an eight-line multiplet.

This is caused by a combination of strong one-bond coupling to the metalated P<sub>O</sub> (<sup>1</sup>*J*<sub>QX</sub> 235.8 Hz), sensible coupling to the phosphorus sulfide P<sub>Z</sub> apex (<sup>2</sup>*J*<sub>XZ</sub> 70.3 Hz), and small coupling to the apical triphos P<sub>A</sub> atom (<sup>3</sup>*J*<sub>XA</sub> 8.3 Hz). No coupling to the two equatorial triphos P<sub>M</sub> atoms is recognizable. Inset c in Figure 1 highlights the metalated P<sub>O</sub> atom which displays a remarkable 36 line multiplet easily computed as a tddt pattern. This is due to large couplings to both P<sub>X</sub> and the trans-disposed triphos P<sub>A</sub> atoms (<sup>2</sup>*J*<sub>QA</sub> 148.9 Hz) and to minor couplings to P<sub>Z</sub> (<sup>2</sup>*J*<sub>OZ</sub> 41.6 Hz) and the two P<sub>M</sub> atoms (<sup>2</sup>*J*<sub>QM</sub> 24.0 Hz). The apical P<sub>Z</sub> atom of the cage, no longer coordinated to the metal, resonates at 85.20 ppm (trace b in Figure 1) thus moving significantly downfield from the free ligand value [ $\Delta = \delta(\text{P}_Z)_2 - \delta(\text{P}_Z)_{\text{P}_4\text{S}_3} = 20.1$  ppm]. The corresponding value for **2** is somewhat larger [ $\Delta = \delta(\text{P}_Z)_2 - \delta(\text{P}_Z)_{\text{P}_4\text{S}_3} = 26.4$  ppm] as it could be expected in view of the coordination of P<sub>Z</sub> to the transition metal. Indirectly, the comparison of the results for **3** and **2** suggests that coordination of P<sub>Z</sub> is not the only cause for the downfield chemical shift. The triphos P<sub>A</sub> and P<sub>M</sub> atoms fall in the expected region and exhibit dt (P<sub>A</sub>) and dd (P<sub>M</sub>) multiplicities, respectively.

Compounds **2** and **3** represent the first documented example of coordination isomers of the P<sub>4</sub>S<sub>3</sub> molecule and are probably obtained through independent reaction pathways which do not share any common intermediate. Remarkably, the composition of the reaction mixture does not change on varying the temperature from –60 to +50 °C (<sup>31</sup>P NMR experiment in sealed NMR tube, CD<sub>2</sub>Cl<sub>2</sub> solution), ruling out the existence of any exchanging process between **2** and **3**. Moreover, the final composition of the product mixture from the reaction between **1** and P<sub>4</sub>S<sub>3</sub> does not depend on the temperature. In fact, the approximate product ratio 1:7 is unchanged when four samples of **1** and P<sub>4</sub>S<sub>3</sub> thermostated in CD<sub>2</sub>Cl<sub>2</sub> were allowed to react completely at different temperatures between –10 and +30 °C. At lower temperature, no reaction occurs as the dissociation of the relatively weak coordinated triflate ligand in **1** is prevented. Such an experimental finding indicates that the two isomers are not related to each other but are independently formed during the reaction via two independent processes.

(23) Below this temperature unspecific broadening of each resonance occurs likely as a consequence of the increased solution viscosity and magnetic field inhomogeneity.

(24) The <sup>31</sup>P NMR spectrum of free P<sub>4</sub>S<sub>3</sub> in CD<sub>2</sub>Cl<sub>2</sub> at room temperature consists of a ZX<sub>3</sub> spin system with the following parameters:  $\delta(\text{P}_Z) = 65.08$ ,  $\delta(\text{P}_X) = 127.33$ , (<sup>2</sup>*J*<sub>XZ</sub> 70.0 Hz). For comparison see also: Di Vaira M.; Peruzzini M.; Stoppioni P. *J. Chem. Soc., Dalton Trans.* **1984**, 359 and references therein.

Table 1.  $^1\text{H}$ ,  $^{13}\text{C}\{^1\text{H}\}$ , and  $^{31}\text{P}\{^1\text{H}\}$  NMR Spectral Data and IR Absorptions for the  $\text{P}_4\text{S}_3$  and  $\text{P}_4\text{Se}_3$  Rhenium(I) Complexes<sup>e</sup>

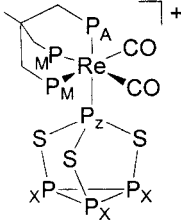
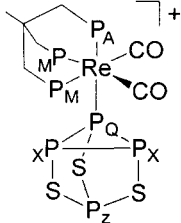
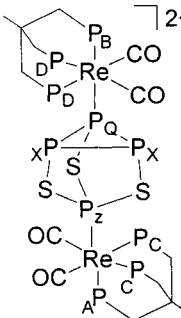
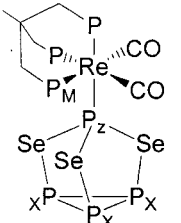
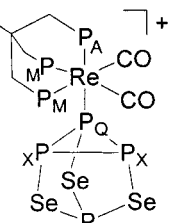
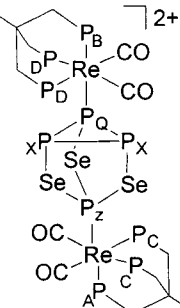
Complexes	$^1\text{H}$	$^{13}\text{C}\{^1\text{H}\}$ <sup>a</sup>	$^{31}\text{P}\{^1\text{H}\}$ $\delta$ (ppm), $J$ (Hz) <sup>b</sup>
	$\delta$ (ppm), $J$ (Hz)	$\delta$ (ppm), $J$ (Hz)	IR (KBr, $\text{cm}^{-1}$ )
 2	1.81 (q, $J_{\text{HP}} = 3.2$ , 3H, $\text{CH}_3$ triphos) 2.48 (m, 2H, $\text{CH}_2\text{P}_M$ ) 2.81 (d, $J_{\text{HP}} = 9.1$ , 2H, $\text{CH}_2\text{P}_A$ ) 2.98 (m, (m, 2H, $\text{CH}_2\text{P}_M$ )	c	$\delta_X -118.61$ (d, $J_{\text{XZ}} = 23.4$ ) $\delta_M -16.92$ (dd, $J_{\text{MZ}} = 25.5$ , $J_{\text{MX}} = 23.4$ ) $\delta_A -13.93$ (dt, $J_{\text{AQ}} = 147.5$ , $J_{\text{AM}} = 25.3$ ) $\delta_Z 91.52$ (dtq, $J_{\text{ZA}} = 147.5$ , $J_{\text{ZM}} = 25.5$ , $J_{\text{ZX}} = 23.4$ ) <sup>d</sup>
 3	1.74 (q, $J_{\text{HP}} = 3.1$ , 3H, $\text{CH}_3$ triphos) 2.68-2.92 (m, 4H, $\text{CH}_2\text{P}_M$ ) 2.72 (d, $J_{\text{HP}} = 10.5$ , 4H, $\text{CH}_2\text{P}_A$ )	193.3 (m, CO) 40.1 (m, $\text{CH}_3$ triphos) 39.1 (m, $\text{CH}_3\text{-C}$ triphos) 36.1 (m, $\text{CH}_2\text{-P}_A$ triphos) 34.3 (m, $\text{CH}_2\text{-P}_M$ triphos)	$\delta_X -134.17$ (ddd, $J_{\text{XQ}} = 235.8$ , $J_{\text{XZ}} = 70.3$ , $J_{\text{XA}} = 8.3$ ) $\delta_Q -44.16$ (tdt, $J_{\text{QX}} = 235.8$ , $J_{\text{QA}} = 148.9$ , $J_{\text{QZ}} = 41.6$ , $\delta J_{\text{QM}} = 24.0$ ) $\delta_M -16.02$ (dd, $J_{\text{MQ}} = 24.0$ , $J_{\text{MA}} = 20.2$ ) $\delta_A -10.66$ (dt, $J_{\text{AQ}} = 148.9$ , $J_{\text{AM}} = 20.2$ , $J_{\text{AX}} = 8.3$ ) $\delta_Z 85.20$ (td, $J_{\text{ZX}} = 70.3$ , $J_{\text{ZQ}} = 41.6$ , $J_{\text{AZ}} = 8.3$ )  $\nu(\text{CO})$ 1973, 1916 $\nu(\text{OTf})$ 1267
 4	1.68 (br s, 3H, $\text{CH}_3$ triphos) 1.79 (br s, 3H, $\text{CH}_3$ triphos) 2.50-3.00 (m, 12H, $\text{CH}_2$ triphos)	193.8 (m, CO) 39.2-41.0 (m, $\text{CH}_3$ triphos + $\text{CH}_3\text{-C}$ triphos) 30.3-36.8 (m, $\text{CH}_2$ triphos)	$\delta_X -126.50$ (dd, $J_{\text{XQ}} = 209.0$ , $J_{\text{XZ}} = 54.1$ ) $\delta_Q -47.60$ (tdt, $J_{\text{QX}} = 209.0$ , $J_{\text{QB}} = 151.9$ , $J_{\text{QZ}} = 21.9$ , $J_{\text{QD}} = 16.2$ ) $\delta_C -16.20$ (dd, $J_{\text{CZ}} = 43.0$ , $J_{\text{CA}} = 25.7$ ) $\delta_A -15.00$ (dt, $J_{\text{AZ}} = 150.8$ , $J_{\text{AC}} = 25.7$ ) $\delta_D -15.00$ (dd, $J_{\text{DB}} = 23.3$ , $J_{\text{DQ}} = 16.2$ ) $\delta_B -12.80$ (dt, $J_{\text{BQ}} = 151.9$ , $J_{\text{BD}} = 23.3$ ) $\delta_Z 93.10$ (dttd, $J_{\text{ZA}} = 150.8$ , $J_{\text{ZX}} = 54.1$ , $J_{\text{ZC}} = 43.0$ , $J_{\text{ZQ}} = 21.9$ )  $\nu(\text{CO})$ 1975, 1921 $\nu(\text{OTf})$ 1267
 5	1.77 (q, $J_{\text{HP}} = 3.1$ , 3H, $\text{CH}_3$ triphos) 2.60-2.90 (m, 6H, $\text{CH}_2$ triphos)	c	$\delta_X -108.74$ (d, $J_{\text{XQ}} = 28.1$ ) $\delta_M -15.27$ (dd, $J_{\text{MQ}} = 24.4$ , $J_{\text{MX}} = 23.2$ ) $\delta_A -13.31$ (dt, $J_{\text{AQ}} = 141.6$ , $J_{\text{AM}} = 23.2$ ) $\delta_Q 91.52$ (dq, $J_{\text{QA}} = 141.6$ , $J_{\text{QX}} = 28.1$ )  c
 6	1.69 (q, $J_{\text{HP}} = 3.2$ , 3H, $\text{CH}_3$ triphos) 2.62-2.90 (m, 4H, $\text{CH}_2\text{P}_M$ ) 2.66 (d, $J_{\text{HP}} = 9.0$ , 2H, $\text{CH}_2\text{P}_A$ )	193.7 (m, CO) 39.9 (q, $J_{\text{CP}} = 9.8$ , $\text{CH}_3$ triphos) 39.7 (m, $\text{CH}_3\text{-C}$ triphos) 34.7 (br t, $J_{\text{CP}_M} = 14.3$ , $\text{CH}_2\text{-P}_M$ triphos) 32.3 (dt, $J_{\text{CP}_A} = 27.4$ , $J_{\text{CP}_M} = 4.1$ , $\text{CH}_2\text{-P}_A$ triphos)	$\delta_X -117.60$ (ddd, $J_{\text{XQ}} = 238.2$ , $J_{\text{XZ}} = 69.5$ , $J_{\text{XA}} = 7.3$ ) $\delta_Q -42.43$ (tdt, $J_{\text{QX}} = 238.2$ , $J_{\text{QA}} = 145.9$ , $J_{\text{QZ}} = 48.8$ , $\delta J_{\text{QM}} = 25.0$ ) $\delta_A -10.80$ (dt, $J_{\text{AQ}} = 145.9$ , $J_{\text{AM}} = 23.2$ , $J_{\text{AX}} = 7.3$ ) $\delta_M -16.20$ (dd, $J_{\text{MQ}} = 25.0$ , $J_{\text{MA}} = 23.2$ ) $\delta_Z 57.56$ (td, $J_{\text{ZX}} = 69.5$ , $J_{\text{ZQ}} = 48.8$ )  $\nu(\text{CO})$ 1973, 1916 $\nu(\text{OTf})$ 1267

Table 1 (Continued)

Complexes	$^1H$	$^{13}C\{^1H\}^a$	$^{31}P\{^1H\}$
	$\delta$ (ppm), $J$ (Hz)	$\delta$ (ppm), $J$ (Hz)	$\delta$ (ppm), $J$ (Hz) <sup>b</sup> IR (KBr, $cm^{-1}$ )
	1.68 (br s, 3H, $CH_3$ triphos) 1.81 (br s, 3H, $CH_3$ triphos) 2.41-3.10 (m, 12H, $CH_2$ triphos)	193.3 (m, CO) 38.9-40.0 (m, $CH_3$ triphos + $CH_3-C$ triphos) 36.7 (tm, $J_{CP} = 13.3$ , $CH_2-P_C$ or D triphos) 34.8 (tm, $J_{CP} = 12.1$ , $CH_2-P_D$ or C triphos) 31.7 (dm, $J_{CP} = 28.6$ , $CH_2-P_B$ or A triphos) 30.7 (dt, $J_{HP_A} = 23.1$ , $CH_2-P_A$ or B triphos)	$\delta_X -110.78$ (dd, $J_{XQ} = 210.0$ , $J_{XZ} = 45.2$ ) $\delta_Q -42.48$ (td, $J_{QX} = 210.0$ , $J_{QB} = 148.3$ , $J_{QD} = 17.2$ , $J_{QZ} = 15.6$ ) $\delta_C -12.03$ (dd, $J_{CZ} = 31.2$ , $J_{CA} = 24.4$ ) $\delta_D -11.92$ (dd, $J_{DB} = 22.5$ , $J_{DQ} = 17.2$ ) $\delta_A -11.88$ (dt, $J_{AZ} = 152.6$ , $J_{AC} = 24.4$ ) $\delta_B -10.00$ (dt, $J_{BQ} = 148.3$ , $J_{BD} = 22.5$ ) $\delta_Z$ 51.58 (dtd, $J_{ZA} = 152.6$ , $J_{ZX} = 45.2$ , $J_{ZC} = 31.2$ , $J_{ZQ} = 15.6$ ) v(CO) 1970, 1916 v(OTf) 1267

7

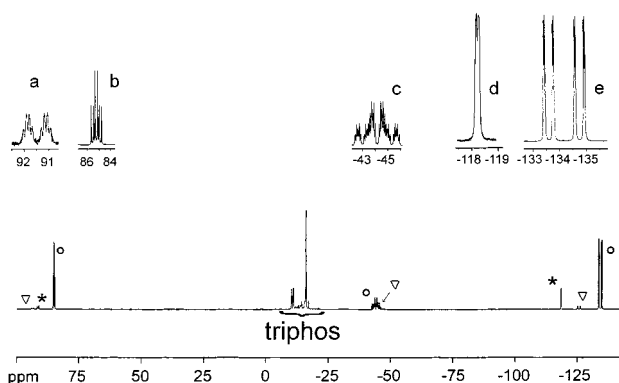
<sup>a</sup> Confirmed by DEPT-135 experiment. <sup>b</sup> All  $^{31}P\{^1H\}$  NMR were confirmed by  $^{31}P\{^1H\}$ -COSY. Key: s, singlet; d, doublet; t, triplet; q, quartet; m, multiplet; br, broad. <sup>c</sup> The  $^{13}C\{^1H\}$  NMR resonances of **3** and **5** could not be safely assigned as both these complexes are formed in very minor concentration and their resonances are likely masked by the most abundant species, and their IR bands could not be assigned for the same reason. <sup>d</sup> Due to the similarities of  $J_{ZM}$  and  $J_{ZX}$  the multiplet appears as a doublet of pseudosextuplets, see text. <sup>e</sup> The NMR spectra were recorded in  $CD_2Cl_2$  at room temperature using Bruker AC200, Varian VXR300, and Bruker Avance DRX500 instruments.

Table 2. Comparison of the  $^{31}P\{^1H\}$  NMR Data for the  $P_4S_3$  and  $P_4Se_3$  Ligands and the Rhenium(I) Complexes

compound	chemical shift, ppm			$J$ , Hz		
	$P_{apical}$ (Pz)	$P_{basal}$ (PQX)		$J_{XZ}$	$J_{QZ}$	$J_{QX}$
$P_4S_3$	65.1	-127.3		70		
$P_4Se_3$	30.7	-114.1		72		

compound	chemical shift, ppm			$J$ , Hz		
	$P_{apical}$ (Pz)	$P_X$	$P_Q$	$J_{XZ}$	$J_{QZ}$	$J_{QX}$
[(triphos)Re(CO) <sub>2</sub> { $\eta^1$ - $P_{apical}$ - $P_4S_3$ }] (OTf) ( <b>2-OTf</b> )	91.52	-118.61		23.4		
[(triphos)Re(CO) <sub>2</sub> { $\eta^1$ - $P_{basal}$ - $P_4S_3$ }] (OTf) ( <b>3-OTf</b> )	85.20	-134.17	-44.16	70.3	41.6	235.8
[(triphos)Re(CO) <sub>2</sub> ] <sub>2</sub> { $\mu, \eta^{1:1}$ - $P_{apical}, P_{basal}$ - $P_4S_3$ }] (OTf) <sub>2</sub> ( <b>4-OTf</b> )	93.10	-126.50	-47.60	54.1	21.9	209.0
[(triphos)Re(CO) <sub>2</sub> { $\eta^1$ - $P_{apical}$ - $P_4Se_3$ }] (OTf) ( <b>5-OTf</b> )	42.76	-108.74		28.1		
[(triphos)Re(CO) <sub>2</sub> { $\eta^1$ - $P_{basal}$ - $P_4Se_3$ }] (OTf) ( <b>6-OTf</b> )	57.56	-117.60	-42.43	69.5	48.8	238.2
[(triphos)Re(CO) <sub>2</sub> ] <sub>2</sub> { $\mu, \eta^{1:1}$ - $P_{apical}, P_{basal}$ - $P_4Se_3$ }] (OTf) <sub>2</sub> ( <b>7-OTf</b> )	51.58	-110.78	-42.48	45.2	15.6	210.0



**Figure 1.**  $^{31}P\{^1H\}$  NMR spectrum in  $CD_2Cl_2$  of [(triphos)Re(CO)<sub>2</sub>{ $\eta^1$ - $P_{apical}$ - $P_4S_3$ }]<sup>2+</sup> (**2**) (\*) and [(triphos)Re(CO)<sub>2</sub>{ $\eta^1$ - $P_{basal}$ - $P_4S_3$ }]<sup>2+</sup> (**3**) (O). The symbol  $\nabla$  denotes a small amount of the dimer **4**.

The IR spectrum (Nujol mull) is scarcely informative and points out the presence of two broad and intense absorptions due to the two equatorial carbonyl ligands of the [(triphos)-Re(CO)<sub>2</sub>]<sup>+</sup> moiety in complex **3**. The absorptions of the minor abundant isomer, **2**, were not distinguished. As a matter of fact, the two CO stretching absorptions of **3** fall

very close to those reported for the [(triphos)Re(CO)<sub>2</sub>( $\eta^1$ - $P_4$ )](OTf),<sup>22</sup> suggesting similar electron donor capabilities toward rhenium(I) for white phosphorus and tetraphosphorus trisulfide.

Compounds **2-OTf** and **3-OTf** are air stable in the solid state and, for a short exposure time, in solution of halogenated solvents, THF, and acetone. They do not dissolve in apolar solvents, diethyl ether, and alcohols. Column chromatography using  $CH_2Cl_2/n$ -hexane (3:1) as eluent enables a separation of the major component **3** from **2**. A pure sample of compound **3-OTf** can also be obtained by careful crystallization from a dilute  $CH_2Cl_2$ /EtOH (5:1) solution. Nevertheless, pure samples of **2-OTf** could not be obtained either through chromatographic methods or through fractional crystallization. Solutions of **3** in  $CH_2Cl_2$  under nitrogen are quite stable and do not re-form **2** over weeks.

**Synthesis and Characterization of the Dinuclear  $P_4S_3$  Sandwich Complex** [(triphos)Re(CO)<sub>2</sub>]<sub>2</sub>{ $\mu, \eta^{1:1}$ - $P_{apical}, P_{basal}$ - $P_4S_3$ }] (OTf)<sub>2</sub> (**4-OTf**). Depending on the stoichiometric ratio between **1** and  $P_4S_3$ , the formation of the two isomers **2** and **3** may be accompanied by that of a third rhenium



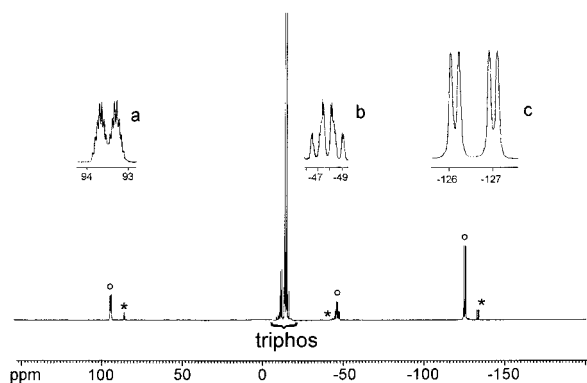


**Figure 2.**  $^{31}\text{P}\{^1\text{H}\}$  NMR spectrum in  $\text{CD}_2\text{Cl}_2$  of  $\{[(\text{triphos})\text{Re}(\text{CO})_2]_2\text{-}\{\mu,\eta^{1:1}\text{-}P_{\text{apical}},P_{\text{basal}}\text{-}P_4\text{S}_3\}\}^{2+}$  (**4**) (O). The asterisk (\*) denotes a small amount of **3**.

derivative, **4** (see Figure 1). The concentration of this latter species increases when the reaction is carried out in less than stoichiometric amount of  $P_4S_3$ , and **4** forms quantitatively when 1 equiv of **1** is purposefully added to a solution of **2** and **3** (Scheme 1). A reasonable explanation is that the added rhenium triflate complex reacts with each of the two coordination isomers **2** or **3** forming the same binuclear species of formula  $\{[(\text{triphos})\text{Re}(\text{CO})_2]_2\{\mu,\eta^{1:1}\text{-}P_{\text{apical}},P_{\text{basal}}\text{-}P_4\text{S}_3\}\}^{2+}$  (**4**). The dimer **4** is therefore quantitatively produced irrespective of the apical or basal coordination mode adopted by the  $P_4S_3$  ligand in the educt species and may be considered as a sandwich complex in which a  $P_4S_3$  molecule is tethering two rhenium(I) fragments. Addition of  $1/2$  equiv of  $P_4S_3$  to a  $\text{CH}_2\text{Cl}_2$  solution of **1** generates **4** in almost quantitative yield.

The two coordination isomers of  $P_4S_3$  do not react with additional **1** with the same speed notwithstanding they both lead to **4**. Thus, when a solution of **2** and **3** (1:7) is treated with 0.2 equiv of **1** in  $\text{CD}_2\text{Cl}_2$  at room temperature, the  $\eta^1\text{-}P_{\text{apical}}$ -isomer, **2**, disappears faster than **3** to yield **4**. The dimerization reaction is irreversible, and once formed the dinuclear species **4** does not re-form **1** after prolonged staying in dichloromethane solution. Conversely, addition of a 10-fold excess of  $P_4S_3$  to a solution of **4** in the same solvent (NMR tube experiment) does not give back any of the two monomers.

In the  $^{31}\text{P}\{^1\text{H}\}$  NMR spectrum of **4**, the complicated  $\{\text{AC}_2\}\{\text{BD}_2\}\{\text{QX}_2\text{Z}\}$  spin system reflects the double metalation of the  $P_4S_3$  molecule  $\{\text{QX}_2\text{Z}$  spin system $\}$  which holds together two nonequivalent triphos subunits  $[\{\text{AC}_2\}\{\text{BD}_2\}$  spin system]. The absence of any discernible long-range coupling between the two triphos subunits and the inspection of the  $^{31}\text{P}\{^1\text{H}\}$ ,  $^{31}\text{P}\{^1\text{H}\}$ -COSY 2D-NMR spectrum helped us to unravel the  $^{31}\text{P}$  NMR spectrum shown in Figure 2. The analysis of the network of correlation peaks involving the two metalated  $P_Q$  and  $P_Z$  atoms as well as the triphos  $P_A$  and  $P_B$  apical resonances in the COSY spectrum was particularly useful to assign the two triphos subunits which fall in a very narrow region between  $-9.5$  and  $-12.8$  ppm.

The examination of the three multiplets due to the  $\mu,\eta^{1:1}\text{-}P_{\text{apical}},P_{\text{basal}}\text{-}P_4S_3$  ligand reveals that the apical cage atom  $P_Z$  appears as a broadly resolved multiplet at  $\delta = 93.10$  (trace

a in Figure 2). The latter has been computed as a dtd pattern which arises from the coupling of  $P_Z$  to  $P_A$ ,  $P_X$ , and  $P_C$  atoms, with  $P_A$  being the trans triphos atom ( $^2J_{AZ}$  150.8 Hz),  $P_X$  the two equivalent, nonmetalated, basal atoms ( $^2J_{XZ}$  54.1 Hz), and  $P_C$  the triphos P atoms lying trans to the CO ligands ( $^2J_{CZ}$  43.0 Hz). A final doubling of moderate magnitude with the opposite metalated  $P_Q$  nucleus halves each component of the multiplet ( $^2J_{QZ}$  21.9 Hz). The  $P_Q$  resonance appears as a tddt multiplet in which comparable values of the two smaller coupling constants ( $^2J_{QZ}$  21.9 Hz,  $^2J_{CQ}$  16.2 Hz) are responsible for the gross appearance of this signal as a triplet of broad quartets (see trace b in Figure 2). The triplet multiplicity originates from large coupling to the two uncoordinated  $P_X$  atoms ( $^1J_{XQ} = 209.0$  Hz), which, in turn, are responsible for the very high field shifted doublet of doublets ( $\delta_X -126.50$ ) presented as trace c in Figure 2.

Although bimetallic  $\{[\text{Ir}(\text{CO})\text{Cl}(\text{PPh}_3)(\mu\text{-}P_4S_3)]_2\}^{25}$  or trimetallic  $\{[\text{Pt}(\text{PPh}_3)(\mu\text{-}P_4S_3)]_3\}^{26}$  clusters containing two or three bridging  $P_4S_3$  molecules, respectively, resulting from the P–P bond activation, are known, **4** is, to the best of our knowledge, the first authenticated complex containing an intact  $P_4S_3$  molecule bridging two transition metal fragments.<sup>27</sup> The tetramer  $[(\text{C}_5\text{H}_5)_4\text{Cr}_4(\text{CO})_9(\text{P}_4\text{S}_3)]$ ,<sup>28</sup> where the skeleton of the original  $P_4S_3$  cage is no longer evident due to the numerous P–P and P–S bond cleavages, has also been described.

**Synthesis and Characterization of Rhenium– $P_4\text{Se}_3$  Derivatives.** The reaction of **1** with  $P_4\text{Se}_3$  was accomplished using the same protocol as for  $P_4S_3$ , the only significant difference being due to the use of a  $\text{CS}_2/\text{CH}_2\text{Cl}_2$  mixture as a solvent in order to increase the solubility of the phosphorus selenide. The results completely parallel those obtained for  $P_4S_3$ , which is not surprising in view of the similar chemistry of the two chalcogen derivatives.<sup>2–5,29</sup> Thus, by treating **1** with  $P_4\text{Se}_3$ , a mixture of the two coordination isomers  $[(\text{triphos})\text{Re}(\text{CO})_2\{\eta^1\text{-}P_{\text{apical}}\text{-}P_4\text{Se}_3\}]^+$  (**5**) and  $[(\text{triphos})\text{Re}(\text{CO})_2\{\eta^1\text{-}P_{\text{basal}}\text{-}P_4\text{Se}_3\}]^+$  (**6**) in approximately a 1:8 ratio is formed. As found for the  $P_4S_3$  system, the shortage of  $P_4\text{Se}_3$  favors the formation of the dimeric species  $\{[(\text{triphos})\text{Re}(\text{CO})_2]_2\{\mu,\eta^{1:1}\text{-}P_{\text{apical}},P_{\text{basal}}\text{-}P_4\text{S}_3\}\}^{2+}$  (**7**). The latter can be

(25) Ghilardi, C. A.; Midollini, S.; Orlandini, A. *Angew. Chem., Int. Ed. Engl.* **1983**, *22*, 790.

(26) Di Vaira M.; Peruzzini M.; Stoppioni P. *J. Chem. Soc., Dalton Trans.* **1985**, 291.

(27) Although the present NMR analysis does not leave doubts to the solution structure of complex **2–4**, our several attempts to grow good quality crystals suitable for an X-ray analysis were frustrated by intrinsic difficulties because fibrous or twinned crystals were regularly obtained. When transparent and well-formed crystals were apparently grown (from diluted  $\text{CH}_2\text{Cl}_2/\text{EtOH}$  mixtures), a fast evaporation of dichloromethane from the selected crystal hampered our attempts to get a crystallographic analysis.

(28) Goh, L. Y.; Chen, W.; Wong, R. C. S.; Karargiosoff, K. *Organometallics* **1995**, *14*, 3886.

(29) Gysling H. J. In *The Chemistry of Organic Selenium and Tellurium Compounds*; Patai, S., Rappaport, Z., Eds.; John Wiley: New York, 1986; Vol. 1., Chapter 18, pp 754–758.

prepared straightforwardly by reacting **1** with a half proportion of P<sub>4</sub>Se<sub>3</sub> or by treating a mixture of **5** and **6** with **1**. Complexes **5**–**7** share with the sulfido analogues most of their chemical and physical properties. However, the three selenido complexes are only moderately air stable and, within 1 h, decompose to an intractable tanned material in a solution of dichloromethane, acetone, or THF unless a protective nitrogen atmosphere is provided. The <sup>31</sup>P NMR properties of **5**–**7** are similar to those of **2**–**4** with the notable difference due to the <sup>77</sup>Se nucleus (<sup>77</sup>Se: *I* = 1/2; 7.2% natural abundance). The occurrence of the <sup>77</sup>Se-isotopomer “<sup>77</sup>Se<sub>1</sub>-P<sub>4</sub>Se<sub>3</sub>” causes each signal of P<sub>4</sub>Se<sub>3</sub> to be flanked by broad bumps due to the <sup>1</sup>J<sub>PSe</sub> coupling.<sup>30</sup> NMR features of **5**–**7** worth mentioning are (i) the almost identical values of the metalated P<sub>Q</sub> atoms in both **6** and **7**; (ii) the closeness of the P<sub>X</sub> and P<sub>Q</sub> chemical shifts for **5**–**7** with those of the P<sub>4</sub>S<sub>3</sub> analogues **2**, **3**, and **4**; and (iii) the larger deviation of the  $\delta$ P<sub>Z</sub> values on passing from the sulfido complexes **2**–**4** to the selenido species **5**–**7**. The latter finding reflects the large difference of the P<sub>Z</sub> chemical shift for P<sub>4</sub>S<sub>3</sub> in comparison to P<sub>4</sub>Se<sub>3</sub> [ $\Delta = \delta(\text{P}_Z)_{\text{P}_4\text{S}_3} - \delta(\text{P}_Z)_{\text{P}_4\text{Se}_3} = 34.4$  ppm] (Table 2).

The coordination chemistry of P<sub>4</sub>Se<sub>3</sub> is still less studied than that of P<sub>4</sub>S<sub>3</sub>, the only well-documented compounds containing the intact P<sub>4</sub>Se<sub>3</sub> molecule being the complexes [(NP<sub>3</sub>)M( $\eta^1$ -P<sub>4</sub>Se<sub>3</sub>)] (M = Ni, Pd).<sup>9</sup> A more or less complete fragmentation of the P<sub>4</sub>Se<sub>3</sub> cage takes place in all the other reactions combining this cage molecule and a transition metal fragment.<sup>2–5,29</sup> In the case of Goh’s tetramer [(C<sub>5</sub>H<sub>5</sub>)<sub>4</sub>-Cr<sub>4</sub>(CO)<sub>9</sub>(P<sub>4</sub>Se<sub>3</sub>)],<sup>31</sup> the original topology is no longer evident as a result of multiple breakages of both P–P and P–Se bonds.

**Theoretical Calculations.** In this section we will discuss some aspects of the electronic structure of the isomers **2** and **3** and the directional features of the basal lone pairs at the P<sub>4</sub>S<sub>3</sub> cage. The simplified models **2m** and **3m**, which consist of three individual PH<sub>3</sub> molecules in place of the tripodal ligand triphos, have been optimized using the DFT method.

Figure 3 reports the optimized structures of **2m** and **3m** as well as that of the free P<sub>4</sub>S<sub>3</sub> cage (C<sub>3v</sub> symmetry). Both complexes have C<sub>s</sub> symmetry with one P–S vector projecting over the bisector of the P–Re–P equatorial angle. Since the X-ray structures of two complexes **2** and **3** are not available, the computed geometric details are particularly important in this case. Thus, the bond distances are directly reported in the drawings of **2m** and **3m**, and a selection of the angular values is given in Table 3.

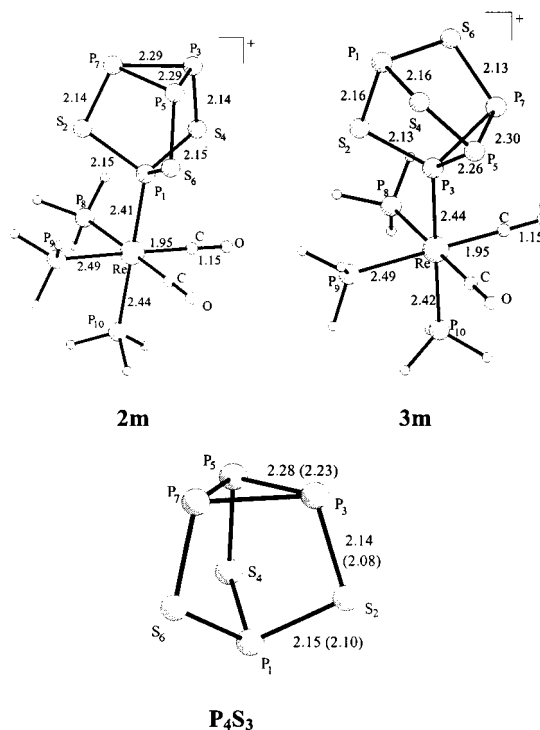


**Figure 3.** Optimized structures of model complexes **2m** and **3m** as well as that of the free P<sub>4</sub>S<sub>3</sub> cage. Distances are given in angstroms (Å); the values in parentheses are the experimental ones from ref 32.

**Table 3.** Relevant Angles (deg) for **2m**, **3m**, and the Free Cage P<sub>4</sub>S<sub>3</sub><sup>a</sup>

	<b>2m</b> (C <sub>s</sub> )	<b>3m</b> (C <sub>s</sub> )	free cage (C <sub>3v</sub> )
P <sub>1</sub> –S <sub>2</sub> –P <sub>3</sub>	101	100	103 (103)
P <sub>1</sub> –S <sub>4</sub> –P <sub>5</sub>	101	103	103 (103)
P <sub>5</sub> –P <sub>3</sub> –P <sub>7</sub>	60	61	60 (60)
S <sub>2</sub> –P <sub>1</sub> –S <sub>4</sub>	101	99	99 (100)
S <sub>4</sub> –P <sub>1</sub> –S <sub>6</sub>	101	100	99 (99)
S <sub>2</sub> –P <sub>3</sub> –P <sub>5</sub>	103	106	104 (103)
S <sub>4</sub> –P <sub>5</sub> –P <sub>3</sub>	104	102	104 (103)
Re–P <sub>1</sub> –S <sub>2</sub>	116		
Re–P <sub>3</sub> –S <sub>2</sub>		118	
Re–P <sub>3</sub> –P <sub>5</sub>		128	
P <sub>8</sub> –Re–P <sub>9</sub>	91	91	
P <sub>8</sub> –Re–P <sub>10</sub>	90	91	
C–Re–C	91	91	

<sup>a</sup> The values in parentheses refer to the experimental X-ray structure of the cage molecule.<sup>32</sup>

Concerning the free cage, it may be seen that the calculated P–P and P–S distances are systematically longer (by ca. 2%) than the experimental ones,<sup>32</sup> given in parentheses. On the other hand, the shape of the cage, when coordinated to the metal, is barely affected in any case. Only a minor compression is calculated for the apical bonding mode (the P–S–P angles in **2m** are ca. 2° smaller with respect to the 103° value of free P<sub>4</sub>S<sub>3</sub>). This is verified also from the available crystal structures of  $\eta^1$ -*P*<sub>apical</sub> metal complexes of P<sub>4</sub>S<sub>3</sub>, e.g., [Mo(CO)<sub>5</sub>( $\eta^1$ -P<sub>4</sub>S<sub>3</sub>)]<sup>6</sup> and [(NP<sub>3</sub>)Ni( $\eta^1$ -P<sub>4</sub>S<sub>3</sub>)]<sup>8</sup> which confirm the close similarity of the free and coordinated cages. In the unprecedented basal coordination, however, the cage appears slightly asymmetric. For instance, the angle P<sub>3</sub>–S<sub>2</sub>–P<sub>1</sub> closes up to 100° whereas the other two P–S–P

(30) The widths of the multiplets of P<sub>Z</sub> and P<sub>Q</sub> in **6** as well as of P<sub>Q</sub> in **7** do not allow a correct estimation of the related <sup>1</sup>J(P,Se) couplings. However, the observation of two featureless bumps, representing the external components of the <sup>31</sup>P NMR resonance in those complexes incorporating one <sup>77</sup>Se-nucleus, close to the signal of P<sub>X</sub> in **6** and of both P<sub>Z</sub> and P<sub>X</sub> in **7**, suggests the occurrence of <sup>1</sup>J(P,Se) values comprised between 480 and 585 Hz. These values broadly match with the wide unpredictability of <sup>1</sup>J(P,Se), which is reported to vary between 200 and 1100 Hz; see: Verkade, J. G.; Quin, L. D. In *Phosphorus-31 NMR Spectroscopy in Stereochemical Analysis*; Verlag Chemie: Weinheim, Germany, 1987; p 453. The solubility of the complexes was not enough to allow us to run reliable <sup>77</sup>Se NMR spectra.

(31) Goh, L. Y.; Chen, W.; Wong, R. C. S. *Phosphorus, Sulfur Silicon Relat. Elem.* **1994**, 93/94, 209. Goh, L. Y.; Chen, W.; Wong, R. C. S. *Organometallics* **1999**, 18, 306.

(32) Leung, Y. C.; van Houten, S.; Vos, A.; Wiegers, G. A.; Wiebenga, E. H. *Acta Crystallogr.* **1958**, 10, 574.

angles remain as open as  $103^\circ$ . Also the  $P_5-P_7$  bond, opposite to the metal-coordinated  $P_3$  atom, is clearly more elongated than its analogues ( $2.30 \text{ \AA}$  vs  $2.26 \text{ \AA}$ ).

The Re–P bond involving the cage is somewhat longer in **3m** than in **2m** ( $2.44 \text{ \AA}$  vs  $2.41 \text{ \AA}$ ) thus suggesting a stronger donor power of the apical P atom with respect to the basal one. Whether coordinated or not, the  $P_{\text{apical}}$  atom of  $P_4S_3$  does not change its pyramidity as the  $S-P_{\text{apical}}-S$  angle is equal to  $100^\circ$  in both **2m** and **3m** (and  $99^\circ$  in the free cage). Finally, the Re–P–S angles are  $116^\circ$  in **2m** while the Re– $P_3$ – $S_2$  one is  $118^\circ$  in **3m**. The difference is minimum although the latter angle is significantly related to the direction of the lone pair donated to the metal (vide infra).

Also from the energetic point of view, the alternative coordination modes of  $P_4S_3$  are quite similar. As a matter of fact, the isomer with the  $\eta^1-P_{\text{apical}}$  coordination is calculated to be only  $2.0 \text{ kcal mol}^{-1}$  more stable than the  $\eta^1-P_{\text{basal}}$  one. Single-point MP2 calculations, performed by using DFT optimized geometries, double the  $\Delta E$  value ( $4.0 \text{ kcal mol}^{-1}$ ) thus confirming the greater thermodynamic stability of **2m**. This is likely attributable to the shorter, hence stronger, Re– $P_{\text{cage}}$  coordination bond ( $2.41$  vs  $2.44 \text{ \AA}$ , in **2m** and **3m**, respectively). In contrast, the experimental observation, that complex **3** is experimentally 7 times more abundant than **2**, can be justified on the basis of pure statistics (3:1 the ratio of existing basal vs apical P donors). After all, the difference in thermodynamic stability of the two species is relatively small and additional MP2 single-point calculations, which include the effect of the dichloromethane solvent, reduce the gap ( $\Delta E = 2.1 \text{ kcal mol}^{-1}$ ).

While the direction of the lone pair at the apical P atom coincides with the 3-fold axis of the cage, it is interesting to comment on the directionality of the basal lone pairs. By adopting the natural hybrid orbital technique (NHO), as implemented in the package Gaussian98,<sup>33</sup> we calculated that, for the free  $P_4S_3$  cage, the direction of maximum electron density pointing out from any basal P atom forms an angle  $\tau$  of  $130^\circ$  with the  $P_3$  plane. In **3m**, the angle formed by Re–P coordination bond is only slightly larger ( $133^\circ$ ). Qualitative MO arguments are helpful in framing the nature of the dative bond departing from one atom of the  $P_3$  ring and its directionality.

The frontier MO region of the free  $P_4S_3$  molecule is characterized by 10 filled levels, which identify with six sulfur and four phosphorus lone pairs (see Figure 4).

The three highest  $3e$  and  $a_2$  levels are uninvolved combinations of the  $p_\pi$  orbitals of the sulfur atoms with

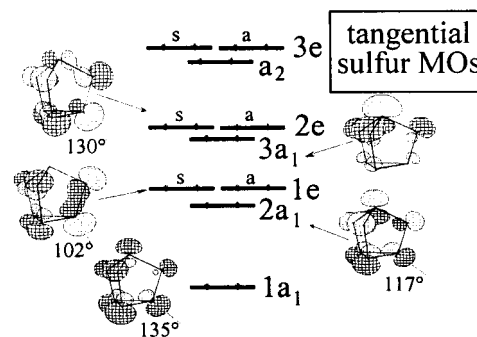


Figure 4. Frontier MO region of the free  $P_4S_3$  molecule.

tangential character with respect to the  $S_3$  triangle.<sup>34</sup> Among the remaining combinations (two of  $e$  type and three of  $a_1$  type), it is not straightforward to distinguish between three sulfur and four phosphorus radial lone pairs as the MOs are distributed quasi homogeneously over the seven atoms (exceptionally,  $3a_1$ , receives minimum contribution from the basal atoms). Thus, at least four MOs (the symmetric components of the two  $e$  sets and those of the two lower  $a_1$  levels) are engaged in the bonding between one basal P atom and the external  $\sigma$  acceptor.

The important lobes of the four  $P_4S_3$  MOs involved in donation are not equally oriented on the basal  $P_3$  plane (see  $\tau$  angles in Figure 4). Eventually, the direction of the donor–acceptor bond is a resultant of four weighted components, the prevailing one being  $2e_s$  which, on account of its highest energy, interacts most with the  $\sigma$  acceptor. Interestingly, the corresponding  $\tau$  angle of  $130^\circ$  matches the value of the NHO. The two lower orbital components are more biased and should contribute to reduce the angular value which is on the contrary greater ( $133^\circ$ ). In actuality, the potential energy curve for reorienting the  $(PH_3)_3(CO)_2Re(I)$  fragment in the  $\tau$  range  $125-140^\circ$  is quite flat ( $\Delta E = 1.4 \text{ kcal mol}^{-1}$  at the DFT level). Also, the P–Re overlap population is practically unchanged. These results are quite intuitive for slightly misaligning a  $\sigma$  orbital about an sp hybrid pointing in its direction.<sup>35</sup>

Along the same lines, the somewhat wider range of the angles between the  $P_3$  ring and one M–P bond departing from it could be discussed for relatable systems. We refer in particular to  $[(NP_3)Ni(\eta^1-P_4)]$ <sup>36</sup> [ $NP_3 = N(CH_2CH_2)PPh_2_3$ ], where the  $\eta^1$ -coordinated  $P_3$  ring is part of a  $P_4$  molecule, or to  $[(\text{triphos})Co\{\eta^3-P_3(W(CO)_5)_2\}]$ ,<sup>37</sup> where the same ring is capped by a metal fragment. In the two latter species, the experimental  $\tau$  angles are  $161^\circ$  and  $143^\circ$ , respectively. A quantitative and qualitative MO analysis of these compounds (to be reported elsewhere)<sup>38</sup> suggests that

(33) Frisch, M. J.; Trucks, G. W.; Schlegel, H. B.; Scuseria, G. E.; Robb, M. A.; Cheeseman, J. R.; Zakrzewski, V. G.; Montgomery, J. A.; Stratmann, R. E.; Burant, J. C.; Dapprich, S.; Millam, J. M.; Daniels, A. D.; Kudin, K. N.; Strain, M. C.; Farkas, O.; Tomasi, J.; Barone, V.; Cossi, M.; Cammi, R.; Mennucci, B.; Pomelli, C.; Adamo, C.; Clifford, S.; Ochterski, J.; Petersson, G. A.; Ayala, P. Y.; Cui, Q.; Morokuma, K.; Malick, D. K.; Rabuck, A. D.; Raghavachari, K.; Foresman, J. B.; Cioslowski, J.; Ortiz, J. V.; Stefanov, B. B.; Liu, G.; Liashenko, A.; Piskorz, P.; Komaromi, I.; Gomperts, R.; Martin, R. L.; Fox, D. J.; Keith, T.; Al-Laham, M. A.; Peng, C. Y.; Nanayakkara, A.; Gonzalez, C.; Challacombe, M.; Gill, P. M. W.; Johnson, B. G.; Chen, W.; Wong, M. W.; Andres, J. L.; Head-Gordon, M.; Replogle, E. S.; Pople, J. A. Gaussian 98, revision A.9; Gaussian, Inc.: Pittsburgh, PA, 1998.

(34) If we consider that each sulfur atom carries also an outpointing  $\sigma$  lone pair, it may not be excluded that an appropriate transition metal fragment which combines  $\sigma$  and  $d_\pi$  acceptor capabilities can achieve the as yet unknown S-coordination of the cage. Possible candidates to the purpose are  $d^8-ML_2$  and  $d^6-ML_4$  transition metal fragments.

(35) Gimarc, B. M. *Molecular Structure and Bonding*; Academic Press: New York, 1979.

(36) Dapporto, P.; Midollini, S.; Sacconi, L. *Angew. Chem., Int. Ed. Engl.* **1979**, *18*, 469.

(37) Di Vaira, M.; Ehses, M. P.; Peruzzini, M.; Stoppioni, P. *J. Organomet. Chem.* **2000**, *593*, 127.

(38) Mealli, C.; Ienco, A.; Peruzzini, M. Unpublished results.



the *P*<sub>basal</sub> sp hybrids are significantly more bent with respect to the *P*<sub>4</sub>*S*<sub>3</sub> analogues. On the other hand, the donor power of each P atom remains almost unchanged.

### Concluding Remarks

This study provides sound experimental evidence that not only the formation of the  $\eta^1$ -*P*<sub>basal</sub> coordination of the *P*<sub>4</sub>*S*<sub>3</sub> and *P*<sub>4</sub>*Se*<sub>3</sub> cages is possible but, at least for the [(triphos)-Re(CO)<sub>2</sub>]<sup>+</sup> system under investigation, it exceeds the  $\eta^1$ -*P*<sub>apical</sub> isomer by a factor of 7 (8 for *P*<sub>4</sub>*Se*<sub>3</sub>). The DFT calculations have permitted detailed description of the structural features of the two isomers, which could not be determined by X-ray diffraction in the lack of suitable diffracting crystals. Moreover, the calculated energy differences between the coordination isomers are rather small, thus suggesting that the prevalence of the basal coordination mode may be simply attributable to statistics. The strength of the basal vs apical lone pair does not seem to be a discriminating factor also in view of the ease by which the contributing donor orbitals can rehybridize, hence change direction.

### Experimental Section

**General Information.** Dichloromethane was purified by distillation under nitrogen over *P*<sub>2</sub>*O*<sub>5</sub>. Carbon disulfide was reagent grade and was used as received. Complex **1** was prepared as described in the literature,<sup>15</sup> and *P*<sub>4</sub>*S*<sub>3</sub> was obtained from Fluka AG and was recrystallized from benzene prior to use. *P*<sub>4</sub>*Se*<sub>3</sub> was prepared from red phosphorus and black selenium as described in the literature<sup>39</sup> and purified by Soxhlet extraction with benzene. Deuterated dichloromethane for NMR measurements (Aldrich) was dried over molecular sieves (4 Å). <sup>1</sup>H, <sup>13</sup>C{<sup>1</sup>H}, and <sup>31</sup>P{<sup>1</sup>H} NMR spectra were recorded on Bruker AC200 or Bruker AVANCE DRX 500 spectrometers operating at 200.13 or 500.13 MHz (<sup>1</sup>H), 50.32 or 125.80 MHz (<sup>13</sup>C), and 81.01 or 202.45 MHz (<sup>31</sup>P), respectively. Peak positions are relative to tetramethylsilane (<sup>1</sup>H and <sup>13</sup>C) or *H*<sub>3</sub>-*PO*<sub>4</sub> 85% with downfield values taken as positive (<sup>31</sup>P). The <sup>31</sup>P,<sup>31</sup>P-2D COSY NMR experiments were conducted on the AVANCE DRX 500 Bruker spectrometer in the absolute magnitude mode using a 90° pulse after the incremental delay. Infrared spectra were recorded as Nujol mulls on a Perkin-Elmer 1600 series FT-IR spectrometer between KBr plates. Mass spectra were recorded on a Hewlett Packard MS Engine HP 5989A. Elemental analyses (C, H, S) were performed using a Carlo Erba model 1106 elemental analyzer.

**Reaction of [(triphos)Re(CO)<sub>2</sub>(OTf)] (1) with *P*<sub>4</sub>*S*<sub>3</sub>.** A dichloromethane solution (30 mL) of **1** (0.50 g, 0.49 mmol) was treated under nitrogen at room temperature with a solution of *P*<sub>4</sub>*S*<sub>3</sub> (0.11 g, 0.49 mmol) in dichloromethane (20 mL) and stirred at room temperature for 1 h. Concentration of the resulting yellow solution under vacuum to ca. 15 mL and addition of *n*-hexane (20 mL) gave pale yellow-colored microcrystals, which were filtered under nitrogen and washed with light-petroleum ether (2 × 5 mL) before being dried under a brisk current of nitrogen. The NMR analysis indicates the formation of a 1:7 mixture of the two coordination isomers **2** and **3**. Yield: 0.52 g, 0.42 mmol (86%). FABMS: 867 (*M*<sup>+</sup> - *P*<sub>4</sub>*S*<sub>3</sub>); 839, 811 (*M*<sup>+</sup> - *P*<sub>4</sub>*S*<sub>3</sub> - *n*CO, *n* = 1–2). C<sub>44</sub>H<sub>39</sub>F<sub>3</sub>O<sub>5</sub>P<sub>7</sub>ReS<sub>4</sub>: calcd C 42.76, H 3.18, S 10.37; found C 42.4, H 3.3, S 10.5.

**Synthesis of [(triphos)Re(CO)<sub>2</sub>]<sub>2</sub>{ $\mu$ , $\eta^{1:1}$ -*P*<sub>apical</sub>,*P*<sub>basal</sub>-*P*<sub>4</sub>*S*<sub>3</sub>}-**(OTf)**<sub>2</sub> (**4-OTf**). Method A (from **1** and *P*<sub>4</sub>*S*<sub>3</sub>).** A degassed solution of **1** (0.50 g, 0.49 mmol) in dichloromethane (30 mL) was brought to reflux, and 0.05 g of *P*<sub>4</sub>*S*<sub>3</sub> (0.23 mmol) dissolved in 20 mL of dichloromethane was added. The addition was completed in 20 min while the solution was refluxed for 30 min under vigorous stirring. Concentration of the solution to ca. 5 mL and addition of *n*-hexane (10 mL) precipitated **4-OTf** as a yellowish green microcrystalline product. The compound was filtered under nitrogen and washed with light-petroleum ether (2 × 5 mL) before being dried under nitrogen. Yield: 0.42 g, 0.19 mmol (81%).

**Method B (from 2/3 and 1).** A solution of **2/3** (0.40 g, 0.33 mmol) in dichloromethane (25 mL) was treated with 1 equiv of solid **1** (0.33 g, 0.32 mmol) and refluxed for 30 min. Workup as above gave **4-OTf** in ca. 75% yield (0.55 g, 0.24 mmol). C<sub>88</sub>H<sub>78</sub>F<sub>6</sub>O<sub>10</sub>P<sub>10</sub>Re<sub>2</sub>S<sub>5</sub>: calcd C 46.93, H 3.49, S 7.12; found C 46.5, H 3.7, S 7.3.

Metathetical reaction of **4-OTf** with NaBPh<sub>4</sub> in CH<sub>2</sub>Cl<sub>2</sub>/EtOH yielded the tetraphenylborate salt [(triphos)Re(CO)<sub>2</sub>]<sub>2</sub>{ $\mu$ , $\eta^{1:1}$ -*P*<sub>apical</sub>,*P*<sub>basal</sub>-*P*<sub>4</sub>*S*<sub>3</sub>}(BPh<sub>4</sub>)<sub>2</sub> (**4-BPh<sub>4</sub>**). C<sub>134</sub>H<sub>118</sub>B<sub>2</sub>O<sub>4</sub>P<sub>10</sub>Re<sub>2</sub>S<sub>3</sub>: calcd C 62.03, H 4.59, S 3.70; found C 61.6, H 4.6, S 3.4.

**Reaction of [(triphos)Re(CO)<sub>2</sub>(OTf)] (1) with *P*<sub>4</sub>*Se*<sub>3</sub>.** A solution of **1** (0.50 g, 0.49 mmol) in dichloromethane (50 mL) was dropwise added to a well-stirred solution of *P*<sub>4</sub>*Se*<sub>3</sub> (0.18 g, 0.49 mmol) in carbon disulfide (20 mL). The resulting yellowish red solution was gently refluxed for 90 min before being concentrated to ca. 10 mL while hot. Cooling down to room temperature and addition of *n*-hexane (10 mL) gave an orange solid, which was filtered under nitrogen and washed with diethyl ether (2 × 5 mL) before being dried under nitrogen. The NMR analysis indicates the formation of a 1:8 mixture of the two coordination isomers **5** and **6**. Yield: 0.57 g, 0.42 mmol (75%). FABMS: 867 (*M*<sup>+</sup> - *P*<sub>4</sub>*Se*<sub>3</sub>); 839, 811 (*M*<sup>+</sup> - *P*<sub>4</sub>*Se*<sub>3</sub> - *n*CO, *n* = 1–2). C<sub>44</sub>H<sub>39</sub>F<sub>3</sub>O<sub>5</sub>P<sub>7</sub>SSe<sub>3</sub>Re: calcd C 38.39, H 2.86, S 2.33; found C 38.8, H 3.0, S 2.0.

**Synthesis of [(triphos)Re(CO)<sub>2</sub>]<sub>2</sub>{ $\mu$ , $\eta^{1:1}$ -*P*<sub>apical</sub>,*P*<sub>basal</sub>-*P*<sub>4</sub>*Se*<sub>3</sub>}-**(OTf)**<sub>2</sub> (**7-OTf**).** On replacing *P*<sub>4</sub>*S*<sub>3</sub> with *P*<sub>4</sub>*Se*<sub>3</sub> in the preparation of **4-OTf**, the corresponding dinuclear complex **7-OTf** was obtained as yellow microcrystals after similar workup. The use of a CH<sub>2</sub>-Cl<sub>2</sub>/CS<sub>2</sub> (1:1) solution was necessary in method A to efficiently dissolve *P*<sub>4</sub>*Se*<sub>3</sub>. Yield: 76% (method A); 70% (method B). C<sub>88</sub>H<sub>78</sub>F<sub>6</sub>O<sub>10</sub>P<sub>10</sub>Re<sub>2</sub>S<sub>2</sub>Se<sub>3</sub>: calcd C 44.17, H 3.29, S 2.68; found C 44.3, H 3.0, S 2.5.

**Computational Details.** The DFT calculations were performed by using the Gaussian98 package.<sup>33</sup> Structural optimizations were carried out at the hybrid density functional theory (DFT) using the Becke's three-parameter hybrid exchange-correlation functional<sup>40</sup> containing the nonlocal gradient correction of Lee, Yang, and Parr (B3LYP).<sup>41</sup> All optimized structures were confirmed as minima by calculation of numerical vibrational frequencies. A collection of Cartesian coordinates and total energies for all of the optimized molecules are available from the authors upon request. The basis set for the Rh atom utilized the effective core potentials of Hay and Wadt<sup>42</sup> with the associated double- $\zeta$  valence basis functions. The basis set used for the remaining atomic species was the 6-31G one with the important addition of the polarization functions (d, p) for all atoms, including hydrogens.

The starting geometry for optimization was derived from known structures<sup>16–18</sup> containing the [(triphos)Re(CO)<sub>2</sub>] fragment or the

(40) Becke, A. D. *Phys. Rev. A* **1988**, *38*, 3098.

(41) Lee, C.; Yang, W.; Parr, R. G. *Phys. Rev. B* **1998**, *37*, 785.

(42) (a) Dunning T. H.; Hay P. J. *Modern Theoretical Chemistry*, Schaefer, H. F., III., Ed.; Plenum: New York, 1976; Vol. 3, p 1. (b) Hay, P. J.; Wadt, W. R. *J. Chem. Phys.* **1985**, *82*, 299.

(39) Stoppioni P.; Peruzzini M. *Gazz. Chim. Ital.* **1988**, *118*, 581.

uncoordinated cage  $P_4S_3$ .<sup>32</sup> Frequency calculations ensured that the obtained points were minima on the potential surfaces. The zero-point energies for the two isomers are essentially equal (0.111 hartree) and were neglected for the comparisons of total energy. Also, single-point MP2 ab initio calculations<sup>43</sup> were performed at the optimized geometries of the models **2m** and **3m**. The effect of the chloroform solvent was calculated using the Isodensity PCM model.<sup>44</sup> The qualitative perturbation theory arguments used to assess the lone pair directionality were developed through the usage of the EHMO method<sup>45</sup> and its graphics representations.<sup>46</sup>

**Acknowledgment.** This work was supported by INTAS (Project 00-0018: "Towards an Ecoefficient Functionalisa-

tion of White Phosphorus") and EC (INCO ERB-IC15CT960746). I.d.I.R. thanks "Ministerio de Ciencia y Tecnologia" (Spain) for a postdoctoral grant.

**Note Added in Proof.** While this paper was being refereed, a comparable theoretical study of the alternative bonding modes between the  $P_4X_3$  unit ( $X = S, Se$ ) and  $\sigma$  acceptor molecules such as  $BI_3$  and  $NbCl_5$  appeared in *Inorganic Chemistry*.<sup>47</sup> Some of these results were somewhat earlier reported in the *Journal of Molecular Modeling*.<sup>48</sup> In agreement with our findings, the energy differences between the apical and basal coordination modes are evaluated to be very small (1–3 kcal mol<sup>-1</sup>).

- 
- (43) Møller, C.; Plesset, M. S. *Phys. Rev.* **1934**, *46*, 618.  
 (44) Foresman, J. B.; Keith, T. A.; Wiberg, K. B.; Snoonian, J.; Frisch, M. J. *J. Phys. Chem.* **1996**, *100*, 16098.  
 (45) (a) Hoffmann, R.; Lipscomb, W. N. *J. Chem. Phys.* **1962**, *36*, 2872.  
 (b) Hoffmann, R.; Lipscomb, W. N. *J. Chem. Phys.* **1962**, *37*, 3489.  
 (46) (a) Mealli, C.; Proserpio, D. M. *J. Chem. Educ.* **1990**, *67*, 399. (b) Mealli, C.; Ienco, A.; Proserpio, D. M. *Book of Abstracts of the XXXIII ICCS*, Florence, **1998**, 510.

IC010559F

- 
- (47) Aubauer, C.; Irran, E.; Klapötke, T. M.; Schnick, W.; Schulz, A.; Senker, J. *Inorg. Chem.* **2001**, *40*, 4956.  
 (48) Aubauer, C.; Klapötke, T. M.; Schulz, A. *J. Mol. Model.* **2000**, *6*, 76.